RSC Advances

ROYAL SOCIETY OF CHEMISTRY

www.rsc.org/advances

A flexible solid-state supercapacitor based on poly(aryl ether ketone)– poly(ethylene glycol) copolymer solid polymer electrolyte for high temperature applications

Ruiqi Na,[a] Pengfei Huo,[b] Xingrui Zhang,[a] Shuling Zhang,[a] Yinlong Du,[a] Kai Zhu,[a] Yaning Lu,[a] Menghan Zhang,[a] Jiashuang Luan[a] and Guibin Wang*[a]

[a] *College of Chemistry, Key Laboratory of High Performance Plastics, Ministry of Education, Jilin University, Changchun, 130012, P. R. China*

[b] *College of Material Science and Engineering, Northeast Forestry University, Harbin 150040, P. R. China*

Abstract

In order to meet the requirement of the high temperature applications, a high thermal stability solid polymer electrolyte is prepared with poly(aryl ether ketone)–poly(ethylene glycol) copolymer (i.e., PAEK-PEG) as a polymer host, $LiClO_4$ as an electrolyte salt. The novel flexible solid-state supercapacitor is then assembled by the resultant solid polymer electrolyte and activated carbon electrodes. The electrochemical properties of the supercapacitor are analyzed over a wide temperature range of 30 ^{o}C-120 ^{o}C. The fabricated supercapacitor has excellent electrochemical performance especially at high temperature (e.g. high specific capacitance of 103.17 F g^{-1} at 0.1 A g^{-1} and an energy density of 6.76 Wh kg^{-1} with a power density of 9.55 W kg^{-1} at 120 ^{o}C). Simultaneously, this solid polymer electrolyte based supercapacitor possess excellent flexible bending properties and outstanding cycle stability of negligible specific capacitance loss after 2000 cycles at various temperature, demonstrating its feasibility as an energy device for the high temperature applications.

Keywords: solid-state supercapacitors, solid polymer electrolyte, high temperature performance, poly(aryl ether ketone), poly(ethylene glycol)

1. Introduction

With the development of society, a new class of flexible and portable energy devices has attracted a great deal of interest for many applications, like wearable electronics, sensor networks and paper-like power electronics.[1-5] The supercapacitor, also called electrochemical capacitor or ultracapacitor,[6-9] is a promising electrochemical power source due to the combined advantages of higher energy density as compared to conventional capacitors, and higher power density as compared to lithium ion batteries.[6,10] What's more, the supercapacitor has been used under high temperatures, such as in military weapons, space applications, and oil drilling, etc.[11,12] In harsh environments, such supercapacitors with solid polymer electrolytes are superior to liquid electrolytes, as they don't require high safety standard encapsulation materials to prevent the leakage of electrolytes in the device, which seriously limits their practical application.[13-15]

The solid polymer electrolytes are used as the key component of flexible electronic device, which are composite systems based on polymer–salt complexes.[16] Most of the literatures on the solid polymer electrolyte have been devoted for applications in lithium-ion batteries and flexible solid-state supercapacitor, including polyethylene oxide (PEO),[17,18] poly(acrylonitrile) (PAN),[19] poly(vinylalcohol) (PVA) and poly(vinylidene fluoride) (PVdF), etc.[20,21] Among these polymer hosts, PEO-based polymer mixed with several lithium salts (such as $LiClO_4$, $LiPF_6$, $LiAsF_6$, $LiBF_4$ and so on) is a good candidate solid polymer electrolyte for various solid -state electronic devices owing to its excellent cation solubility and a wide electrochemical stability window.[22,23] The mobility of the Li cation is related to the ether oxygen atoms on the amorphous segments of the PEO chain with the breaking/forming lithium–oxygen (Li–O) bonds.[22] Polyethylene oxide is also named as Polyethylene glycol (PEG) when a molecular weight below 20000 g mol^{-1}, which is a kind of polymer with better ionic conductivity due to the lower viscosity of PEG and higher ionic mobility of lithium ions.[22,24] However, the ionic conductivity of PEG based polymer electrolyte is still low at room temperature due to the high degrees of crystallization of the PEG, and the melting point below room temperature also make PEG present some poor mechanical

strength and dimensional stability, which greatly restricts its applications especially in high temperature applications.[17,18,22,23] Among them, the modification methods of PEG based polymer electrolyte was focused mainly on improving the ionic conductivity of polymer electrolyte by suppressing the percentage of the crystallinity phase of PEG while maintaining the dimensional stability especially under high temperature.[25,26] Various approaches were considered such as the addition of the nano-size fillers,[22] polymer blends[27] or plasticizer,[28] designing a PEG based copolymer like liner PEG copolymers,[29,30] grafting PEG oligomers onto other polymer backbones,[31,32] and cross-linked network polymers.[33] The strategie of liner PEG copolymer is an effective way to enhance the ionic conductivity of the PEG based solid polymer electrolyte. Most researches of the solid polymer electrolyte were focused on aliphatic copolymers, such as polyethylene-b-PEO (PE-PEO),[34] polyisoprene-b-PEO (PI-PEO)[35] and polystyrene-b-PEO (PS-PEO).[36] However, the thermal stability and mechanical properties of aliphatic polymer are still poor (usage temperature is lower than 100 ^{o}C) which limit their practical applications in high temperature. Poly(aryl ether ketone) (PAEK) copolymer as a kind of high performance engineering thermoplastics with outstanding thermal stability and mechanical properties,[37,38,39] have been used in lithium batteries,[37] fuel cells[38] and supercapacitors.[40,41] For example, Lu et al. used poly(ethylene oxide) segmented polysulfone copolymers for lithium batteries which the addition of a polysulfone section to improve mechanical performance.[37] Very recently, we reported novel quarternary ammonium functionalized poly(arylene ether sulfone)/ poly(vinylpyrrolidore) composite membranes for separators and composite polymer electrolytes of supercapacitors,[43,44] however, the aqueous electrolyte (6 M KOH) exist some shortcomings for commercial SCs due to its narrow voltage windows and poor performance in high temperature applications. Therefore, development of the solid polymer electrolyte based on PAEK-PEG copolymers is an efficient way to improve the thermal stability and mechanical properties of aliphatic polymer.

With this perspective considering, a series of poly(aryl ether ketone)–poly(ethylene glycol) copolymer with different content of PEG were synthesized. The introduction

of the PAEK segment into the PEG significantly enhanced the thermal stability and mechanical properties of copolymers, and decreased the crystallization of the PEG chain. Meanwhile, the existence of the PEG segment maintained the ionic conductivity of the PAEK-PEG copolymer membrane. The poly(aryl ether ketone)–poly(ethylene glycol) copolymer with the suitable thermal stability and mechanical properties was selected, then the solid polymer electrolyte was produced by dissolving the PAEK-PEG copolymer and $LiClO_4$ in dimethylacetamide, $LiClO_4$ was chosen because $LiClO_4$ has strong electrochemical stability and excellent ionic conductivity in a PEG-based polymer matrix.[19,23] Simultaneously, the resultant solid polymer electrolyte was employed in the fabrication of the high temperature flexible solid-state supercapacitor with activated carbon-based electrodes. The electrochemical properties of the supercapacitor were investigated by using cyclic voltammetry (CV), galvanostatic charge-discharge (GCD), and electrochemical impedance spectroscopy (EIS) techniques under various temperatures. To our knowledge, there have been no similar reports on this type of flexible solid-state supercapacitor with PAEK–PEG based solid polymer electrolyte thus far.

2. Experimental

2.1 Materials

4,4-Difluorobenzophenone (DFBP) was purchased from Changzhou Huashan Chemical Co. Ltd., China. 3,3,5,5-Tetramethyl-4,4-bisphenol (TMBP) was obtained from Shanghai Jiachen Chemical Company. Polyethylene glycol (M_n=1000), thionyl chloride ($SOCl_2$), polytetrafluoroethylene (PTFE) preparation (60 wt% dispersion) and lithium perchlorate ($LiClO_4$, purity: 99.9%) were all bought from Aladdin reagent Co., Ltd. Shanghai, China. Activated carbon (AC) powders (porous volume: 0.7 mL g^{-1}, surface area: 1600 m^2 g^{-1}) and Ketjenblack were obtained from SCM Industrial Chemical Co. Ltd. Shanghai, China. Foamed Nickel was supplied by Lizhiyuan Sales Dept. of batteries, Taiyuan, China. All other chemicals like potassium carbonate (K_2CO_3), tetramethylene sulfone, dimethylacetamide (DMAc) were used from commercial sources and without further purification.

2.2 Synthesis of poly(aryl ether ketone)–poly(ethylene glycol) copolymers

The PAEK–PEG copolymers with different content of PEG were synthesized by a typical synthetic procedure.[42] The schematic of PAEK-40% PEG (the molar ratio of PEG is 40%) synthesis procedure is followed on Scheme 1: under nitrogen atmosphere, TMBP (5.8154 g, 0.024 mol), DFBP (3.1420 g, 0.0144 mol), chlorine-end-capped PEG (9.95 g, 0.0096 mol), potassium carbonate (K_2CO_3, 3.9 g, 0.0288 mol), tetramethylene sulfone (50.10 mL) and toluene (25 mL) were added into a 100 mL three-neck flask with an overhead mechanical stirrer and a Dean-Stark trap with a condenser. The reaction mixture was heated to 130 ^oC and held for 3 h to remove the water from the solution, then the toluene was removed and the temperature was raised to 180 ^oC and continued for 6 h until the very viscous reaction mixture was obtained. The cooling viscous solution was then poured into deionized water to precipitate flexible threadlike copolymer. The copolymer was washed with hot distilled water and hot alcohol for several times, respectively. The PAEK-40% PEG polymer was dried at 100 ^oC in the vacuum oven for 48 h and the product was obtained.

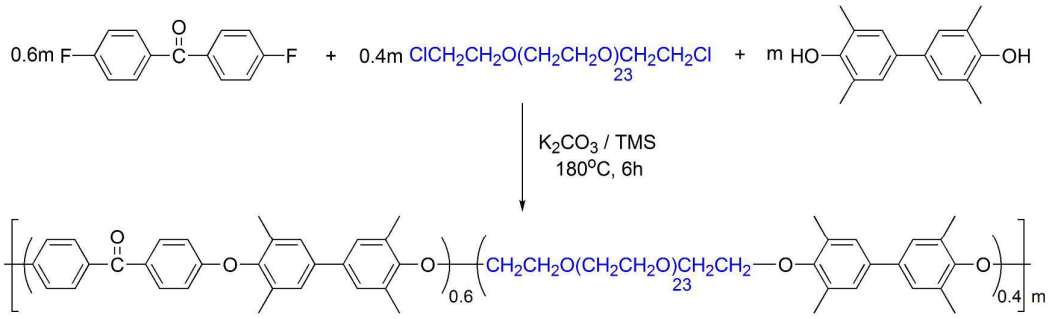

Scheme.1. Synthesis of PAEK– 40%PEG copolymer.

2.3 Preparation of PAEK-x% PEG membranes

To optimize the PEG composition ration onto a PAEK-PEG based polymer matrix, the poly(aryl ether ketone)– poly(ethylene glycol) copolymers with different content of PEG were dissolved in DMAc at a concentration of 0.1 g mL^{-1} and continuously

stirring for 1 h at room temperature until the polymer dissolved completely. Then the solution was poured onto a clean flat glass plate and dried under vacuum at 60 ^{o}C for 12 h, 80 ^{o}C for 12 h and 100 ^{o}C for 12 h. the membranes were denoted as PAEK-x% PEG (x=20, 30, 40, 50, 60).

2.4 Preparation of PAEK-PEG based solid polymer electrolyte

The desired solid polymer electrolyte was prepared according to the following method: the most suitable PAEK-40%PEG copolymer was dissolved in DMAc at a concentration of 0.1 g mL^{-1} and continuously stirred for 30 min at room temperature, then the $LiClO_4$ was dissolved in the solution at a various EO：Li ratio of 8, 10, 12, 14, 16.[22,23] After continuous mechanical stirring at room temperature for 3 h, the homogeneous solution was cast onto a clean flat glass plate and evaporated the solvent at 60 ^{o}C for 12 h, 80 ^{o}C for 12 h and 100 ^{o}C for 12 h in a vacuum oven to obtain the completely dried polymer electrolyte membranes. The thickness of the membrane was around 100 μm, and the optimized solid polymer electrolyte membrane was applied to fabricate flexible all-solid-state supercapacitor.

2.5 Fabrication of flexible solid-state supercapacitor with activated carbon-based electrodes

The AC electrodes were prepared by activated carbon (80 wt%), Ketjenblack (10 wt%) and PTFE (10 wt%) as depicted in our previous work, and the weight of each electrode was measured around 6 mg.[40, 41] Prior to fabricating supercapacitor, two pieces of AC composite electrode films were immersed in DMAc solution at room temperature for 1 min to ensure the wet state of electrodes. The flexible all-solid-state supercapacitor was fabricated with two symmetric AC flexible electrodes, sandwiching a piece of PAEK-40% PEG-$LiClO_4$ solid polymer electrolyte under stress to ensure close contact, i.e. (AC electrode // PAEK-40% PEG-$LiClO_4$ // AC electrode).

2.6 Characterization

2.6.1 Sample analysis

The chemical structure of PAEK-40% PEG copolymer was confirmed by ^{1}H NMR on a Bruker 510 NMR spectrometer (300 MHz) using $CDCl_3$ as solvents and tetramethyl-silane as internal reference. The crystallisation behavior of the PAEK-x% PEG membranes were investigated by X-ray diffraction (XRD) with Rigaku D/max-2500 diffractometer, and Cu Kα radiation as the X-ray source.

2.6.2 Thermal stabilities, mechanical properties and morphologies of pure PAEK-PEG membranes and PAEK-PEG-$LiClO_4$ polymer electrolytes

Thermo gravimetric analysis (TGA) was employed to assess the thermal stability of PAEK-PEG and PAEK-PEG-$LiClO_4$ membranes with Pyris 1TGA (Perkin-Elmer). All the samples were dried and kept in the furnace of TGA at 110 ^{o}C for 20 min under a nitrogen atmosphere using a hating rate of 10 ^{o}C min^{-1}. The mechanical properties of dry membranes were measured at room temperature at a strain rate of 2 cm min^{-1} on SHIMADZUAG-I Universal Tester. The membranes test samples were cut into 25 mm length and 5 mm width. Further, the surface and cross-section morphologies of PAEK-PEG membranes and PAEK-PEG-$LiClO_4$ polymer electrolyte were investigated by SHIMADZU SSX-500 scanning electron microscope (SEM), all the membranes were previously sputter-coated with thin layer gold.

2.6.3 Ionic conductivity study

The ionic conductivity of PAEK-40% PEG-$LiClO_4$ solid polymer electrolyte were carried out in the temperature range of 20 ^{o}C to 170 ^{o}C using electrochemical workstations (CHI660A, Shanghai). The ionic conductivity (σ, S cm^{-1}) of the solid polymer electrolyte was calculated by the following formula (1):

$$\sigma = L / (R_b \times S) \quad (1)$$

where L (cm) is the thickness of the solid polymer electrolyte, S (cm^2) denotes the effective area of polymer electrolyte, R_b (ohm) is the bulk resistance extrapolated from the plateau at high frequency in the real impedance data. Impedance measurements were taken at a frequency range of 100 kHz–1 Hz and the AC amplitude was 10 mV.

For each sample, the average value was measured for three times.

2.6.4 Electrochemical characterization of flexible solid-state supercapacitor

The electrochemical performance of flexible solid-state supercapacitor was analyzed at different temperature (30 ^{o}C, 60 ^{o}C, 90 ^{o}C and 120 ^{o}C). The electrochemical measurements of the supercapacitor were investigated by cyclic voltammograms (CVs) within a stable potential window (0-1.5V) at different scan rates (5-50 mV s^{-1}), the electrochemical impedance spectroscopy (EIS) measurements with an AC potential amplitude of 10 mV and a frequency range from 100 kHz to 0.01 Hz, galvanostatic charge–discharge (GCD) techniques within the stable potential window at different current densities (0.1, 0.2, 0.5, 0.8, 1A g^{-1}) using electrochemical workstations (Model: CHI660A, Shanghai Chen Hua Co., Ltd and LAND, Wuhan, China). The specific capacitance (C_s, F g^{-1}) of the electrodes can be calculated from GCD curves according to the following formula (2):

$$C_s = 4I/[(m \times (\Delta V/\Delta t)] \quad (2)$$

Energy density (E, Wh kg^{-1}) and power density (P, kW kg^{-1}) are also two important parameters for evaluating the electrochemical behaviour of the supercapacitor were evaluated according to the equation (3) and (4):

$$\mathrm{E} = [C_s \times (\Delta V)^2/8] \times (1000/3600) \quad (3)$$

$$\mathrm{P} = E/\Delta t \quad (4)$$

Where I (A) is the constant current, m (g) is the total active mass of two electrodes, ΔV (V) is the operating voltage of the supercapacitor and Δt (s) is the discharge time. The flexible properties and the durability performance of the flexible solid-state supercapacitor at high temperature were also researched and discussed.

3. Results and discussion

3.1 Structure characterization of PAEK- PEG copolymer

The poly(aryl ether ketone)–poly(ethylene glycol) copolymer was synthesized by nucleophilic substitution polycondensation reaction, and the structure of the PAEK-PEG copolymer was confirmed by ^{1}H NMR. Fig. 1(a) shows the ^{1}H NMR

spectrum of PAEK-40%PEG copolymer with $CDCl_3$ as the solvent. The low-field resonance peaks (from 8.0 to 6.5 ppm), 2.2 and 2.3 ppm are asigned to aromatic protons in PAEK unit (a, b, c, d and d'), the PEG chain resonance peak are observed at 3.5–4.0 ppm (e, f and g), which indicates that the PAEK-40% PEG copolymer was synthesized successfully.

The XRD patterns of the PAEK-x% PEG (x=20, 30, 40, 50, 60) copolymer membranes are depicted in Fig. 1(b**)**. The XRD spectrograms of all the samples show a large diffusion peak at $2\theta=20.4^{o}$, the broad diffusion peak indicates the amorphous state of the copolymer. As mentioned above, PEG is a semi-crystalline polymer and only the amorphous phase aids ion transportation.[23] From the results of XRD, ones can find that the amorphous section of the PAEK polymer suppress the crystallinity of the PEG section in the copolymer structure.

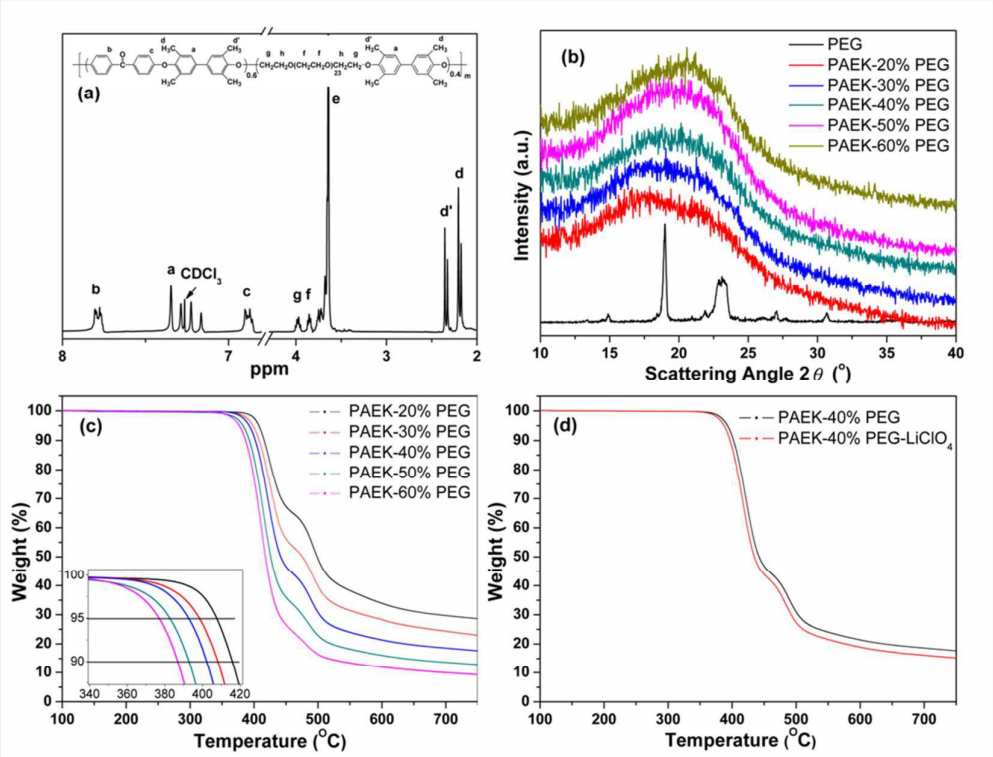

Fig. 1. (a) ^{1}H NMR spectra of PAEK-40% PEG copolymer and (b) WAXD patterns and (c) TGA curves of pure PAEK-x%PEG membranes (x=20, 30, 40, 50 and 60) and (d) comparison of thermal stability of the PAEK-40%PEG membrane and PAEK-40%

PEG-$LiClO_4$ solid polymer electrolyte.

3.2 Thermal stability, mechanical properties and morphologies of PAEK-PEG membranes and solid polymer electrolyte

As a solid polymer electrolyte, thermal stability is critical for energy device in order to meet the requirement of the high temperature applications. The thermal stability of the pure PAEK-PEG polymer membranes and the solid polymer electrolyte membrane were evaluated by TGA under N_2 atmosphere at a rate of 10 ^oC min^{-1}. Fig. 1(c) shows the TGA curves of PAEK-x%PEG (x=20, 30, 40, 50, 60) membranes. As can be seen, all the samples exhibit excellent thermal stability (decomposition temperature >340 °C), and all the TGA curves have two stage of weight loss. The initial weight loss observed around 340 ^oC corresponds to the degradation of the PEG chain, while the second step starting at 442 ^oC and ending at exceed 700 ^oC correspond to the residue of the copolymer matrix. The temperature where the membrane loses 5% weight ($T_{5\%}$) is always used to evaluate the stability of membrane, and the curves of $T_{5\%}$ are shown in the inset of Fig. 1(c). The $T_{5\%}$ of PAEK-x%PEG (x=20, 30, 40, 50, 60) are 407, 398, 392, 382 and 377 ^oC, respectively. It can be seen that the thermal stability of copolymer decreases with the increasing content of PEG. The comparison of thermal stability of the PAEK-40%PEG membrane and addition of moderate $LiClO_4$ salts to form solid polymer electrolyte membrane (PAEK-40% PEG-$LiClO_4$) were also investigated and the results are presented in Fig. 1(d), the changing trend of solid polymer electrolyte is nearly same to PAEK-40%PEG membrane, but the first weight loss degree of PAEK-40% PEG-$LiClO_4$ is a little higher than that of pure membrane, which is probably because the degradation of $LiClO_4$ salts ranging from 380 ^oC to 400 ^oC. The results of TGA indicated that both the pure PAEK-PEG polymer membrane and solid polymer electrolyte had excellent thermal stability.

The tensile strength and elongation at break of the pure polymer membranes and solid polymer electrolyte membrane are summarized in Table 1. It could be seen that the tensile strength of the pure polymer membrane vary in the range of 29.8-1.3 MPa

and the elongation at break of polymer membrane in the range of 159.8-1573.3%. As the increasing content of PEG, the tensile strength of the polymer membrane decreases continuously due to the high flexibility of PEG chains, and the elongation at break reaches a maximum as the mole ratio of PEG is 40%, beyond this point the tensile strength and elongation at break decreases sharply with the content of PEG increasing, for example, the tensile strength and elongation at break of PAEK-50%PEG decreased to 2.5 MPa and 375.3%, respectively. This phenomenon should be ascribed that when the content of PEG chains was higher than 40%, the PEG chain gradually act as mainly component of the membrane and the nature of PEG gradually exhibited in the copolymer, which directly leads to the mechanical property loss. As we all know, the appropriate polymer electrolyte film should maintain not only outstanding electrochemical properties, but also thermal stability and good self-standing behavior, hence the PAEK-40%PEG can be selected as a desired polymer electrolyte matrix. Especially, the solid polymer electrolyte PAEK-40% PEG-$LiClO_4$ also showed enhanced mechanical properties with tensile strength of 12.2 MPa and elongation at break of 467.4%, the elongation at break decreases due to the introduction of small molecule $LiClO_4$ salts. Even so, the mechanical property of polymer electrolyte is still good enough for applications.

Furthermore, the mechanical properties of the membranes are closely related to their morphologies, so we investigated the morphologies of membranes by SEM. Fig.2 shows SEM images of pure PAEK-40%PEG membrane and PAEK-40%PEG-$LiClO_4$ solid polymer electrolyte. According to Fig.2, it can be seen that there are nonporous on both surface and cross-section of PAEK-40%PEG membrane and PAEK-40%PEG-$LiClO_4$ solid polymer electrolyte, and the enhanced mechanical properties of pure PAEK-40%PEG membrane and PAEK-40%PEG-$LiClO_4$ solid polymer electrolyte can also be attributable to the non-pores structure of the membrane.

Table 1. The mechanical properties and sample description 5% ($T_{5\%}$) of polymer membranes and solid polymer electrolyte.

Sample name	Tensile strength (MPa)	Elongation at break (%)	$T_{5\%}$[a] (^{o}C)
PAEK-20%PEG	29.8	159.8	407
PAEK-30%PEG	13.8	469.5	398
PAEK-40%PEG	9.8	1573.3	392
PAEK-50%PEG	2.5	375.3	382
PAEK-60%PEG	1.3	306.7	377
PAEK-40%PEG-$LiClO_4$	12.2	467.4	385

[a] $T_{5\%}$ (^{o}C): 5% weight loss temperature in TGA test.

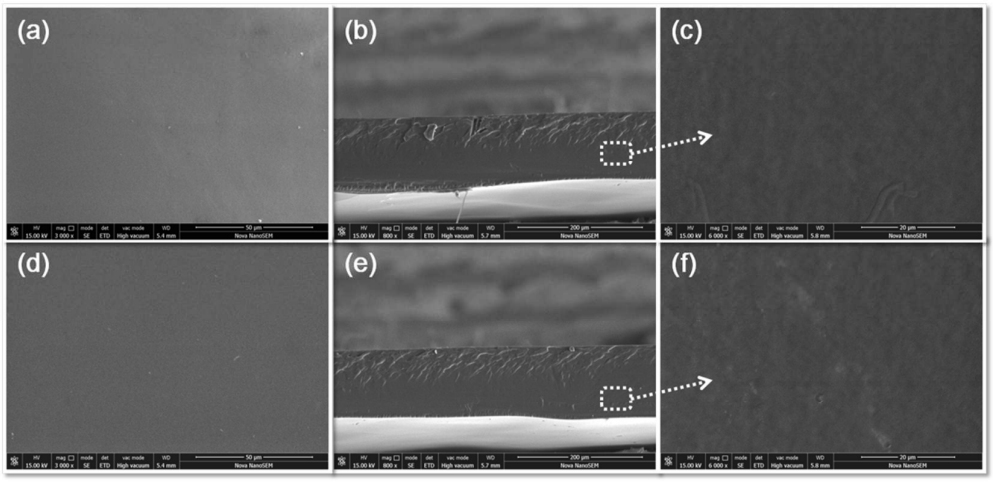

Fig.2. (a) The SEM surface micrograph; (b), (c) cross-section images of pure PAEK-40% PEG membrane and (d) the SEM surface image; (e), (f) cross-section images of PAEK-40% PEG-$LiClO_4$ polymer electrolyte.

3.3 The ionic conductivity of PAEK-40% PEG with $LiClO_4$ solid polymer electrolyte

The temperature-dependent conductivity (from 20 ^{o}C to 140 ^{o}C) for PAEK-40% PEG solid polymer electrolytes with various $LiClO_4$ content (EO: Li=8, 10, 12, 14, 16) are depicted in Fig. 3. Obviously, the ionic conductivities of all the polymer electrolytes rise quickly with increasing temperature,[43, 44] and the plots of the ionic conductivity are non-linear, it was confirmed that their conductivities follow the

Vogel–Tamman–Fulcher (VTF) equation.[45-47] This non-linear VTF behavior is mainly attributed to the complexing segments of the amorphous PEG chain with Li ions, which assisted ions transport through the polymer electrolyte membrane rather than the pores of polymer electrolyte membrane, also, this phenomenon can also be seen in Fig.2 (d)-(e). Besides, the ionic conductivity of PAEK-40% PEG solid polymer electrolytes also increases as the EO: Li ratio decreasing, and reaches the maximum value of 2.6×10^{-4} S cm^{-1} at 30 ^{o}C with the EO: Li =10, in the latter case the ionic conductivity decreases as the EO: Li=8, which is reasonable that with the $LiClO_4$ concentration increases, the valid ions in the polymer host also increased, however, too high $LiClO_4$ concentration (EO: Li=8) lead to the salt crystallites, which impeded the local solubility of the lithium salt in the polymer. Furthermore, high lithium salt content also result in poor mechanical strength which make the PEO-based polymer electrolyte unable to be produced.[48,49] Therefore, the most moderate solid polymer electrolyte is obtained for PAEK-40%PEG copolymer matrix with EO: Li=10.

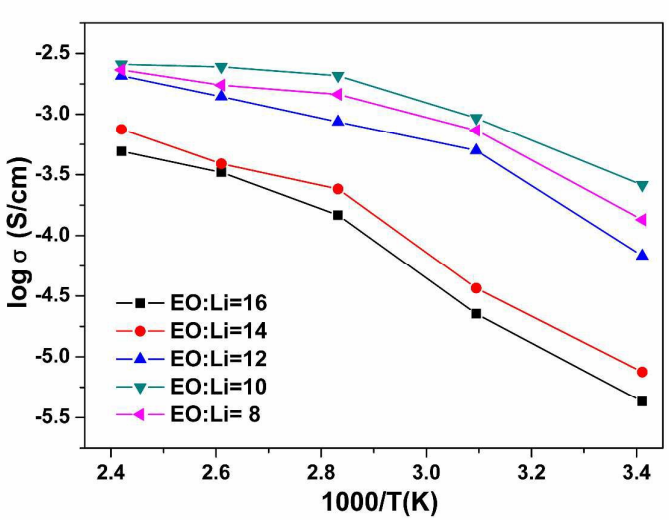

Fig. 3. The ionic conductivity of solid polymer electrolyte at different temperature.

3.4 Electrochemical performance of flexible solid-state supercapacitor

The electrochemical performance of the flexible solid-state supercapacitor based on PAEK-40% PEG-$LiClO_4$ polymer electrolyte with two facing AC electrodes sandwiching was investigated at different temperature. Fig. 4(a) shows the optical

photograph of flexible solid-state supercapacitor and Fig. 4(b) shows the schematic diagram of the Li cations transport by complexation in the segments of the PEG matrix. Before the test, the solid-state supercapacitor was stored at desired temperature for 4 hours.

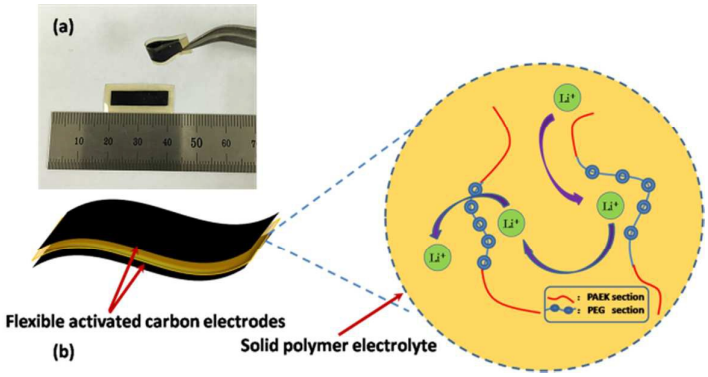

Fig. 4. (a) The optical photograph of the flexible solid-state supercapacitor and (b) the schematic diagram of the supercapacitor using the solid polymer electrolyte.

In order to validate the electrochemical performance of the flexible solid-state supercapacitor, the cyclic voltammograms at different temperature were tested. Fig. 5 shows the CVs of all solid-state supercapacitor measured over a wide range of temperature (30 ^{o}C, 60 ^{o}C, 90 ^{o}C, and 120 ^{o}C, respectively) and with the scan rates in the range of 5–50 mV s^{-1}. The obtained cyclic curves have nearly rectangular shapes with slight variations over a wide range of temperature from 60 ^{o}C to 120 ^{o}C, even at high scan rate, the shapes of CVs remains close to rectangular ones. With increasing temperature, the shapes of cyclic voltammograms are found more similar to rectangular, revealing the ideal capacitive behavior of supercapacitor due to the good migration of charge between the electrode and the solid polymer electrolyte,[50] and higher ionic conductivity at high temperature of solid polymer electrolyte also reduce the sequivalent series resistance and facilitates migration of ions towards electric double layer. In contrast, the rectangular voltammograms get deviations to leaf-like shape at 30 ^{o}C, especially at high scan rate of 50mV s^{-1}, implying higher intrinsic resistance of the supercapacitor which attributed to slower ion diffusion during

electrochemical charge/discharge.

The electrochemical impedance spectroscopy is a very important tool for evaluating the electrochemical behaviour at the electrode/electrolyte interface of the supercapacitor. Fig. 6 illustrates the Nyquist plots at different temperature, respectively. It can be seen that all the shapes of the impedance plots at different temperature are almost the same, which represent that the supercapacitor at various temperature exhibit similar electrochemical capacitance behavior. In the EIS curves, a small semicircle at high frequency region, a straight line inclined at an angel of 45^{o} at middle frequency and a vertical line from middle frequency to low frequency indicating the ideal capacitor of supercapacitor under various temperature.[51] Additionally, the variation of the supercapacitor performance at different temperature can be compared by the intercept on the real axis (Z') at high frequency, which suggests the ohmic resistance of the electrolyte and the internal resistance of the electrode materials and is represented as R_s, and the diameter of semicircle is modeled by an interfacial charge transfer resistance (R_{ct}), with the increase of the temperature, the value of R_s and R_{ct} are decreased significantly, the decrease is mainly due to the enhanced ionic conductivity of the solid polymer electrolyte, and it is verified by Fig. 3.

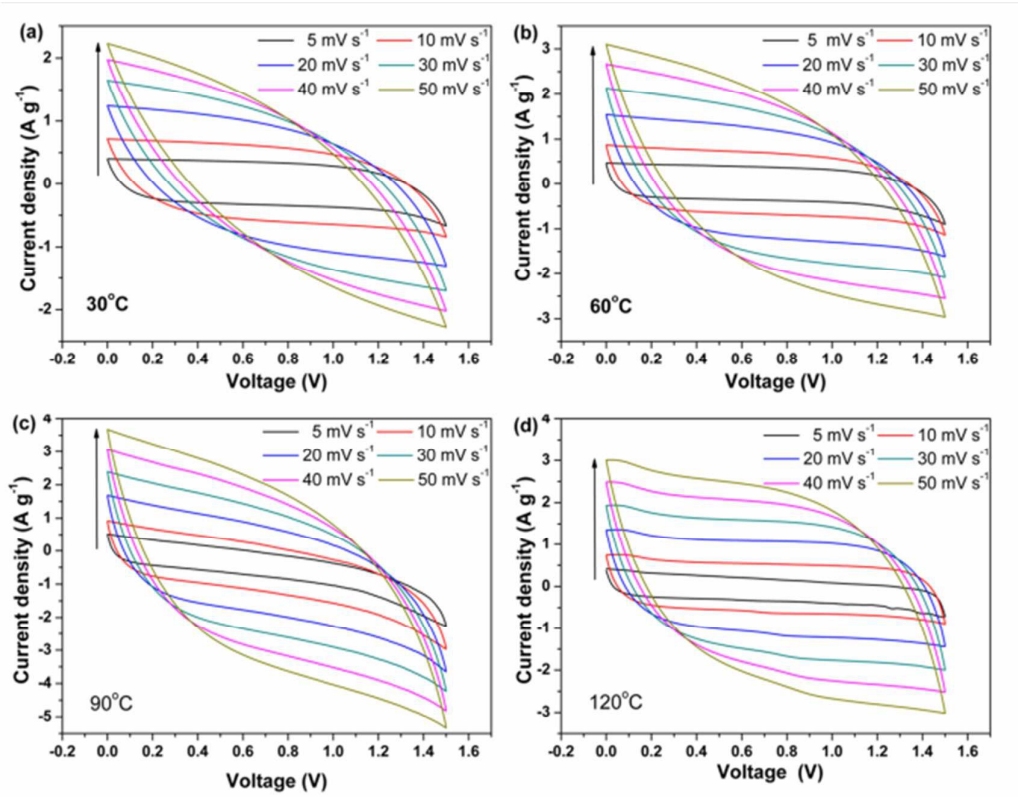

Fig. 5. Cyclic voltammograms of solid-state supercapacitor measured at (a) 30 ^{o}C, (b) 60 ^{o}C, (c) 90 ^{o}C and (d)120 ^{o}C and different scan rates.

Galvanostatic charge–discharge (GCD) test for the solid polymer electrolyte based supercapacitor was investigated at various current densities with different temperature. Fig. 7 (a) shows charge–discharge curves at different current densities at 120 ^{o}C, all these profiles are nearly symmetrical triangles with small voltage drop even at high current densities, further verifying an ideal capacitive behavior of the supercapacitor, the small voltage drop indicates that the overall internal resistance of the device is low, which is important for the practical application. The charge-discharge curves at a current density of 0.2 A g^{-1} at different temperature are shown in Fig. 7 (b).

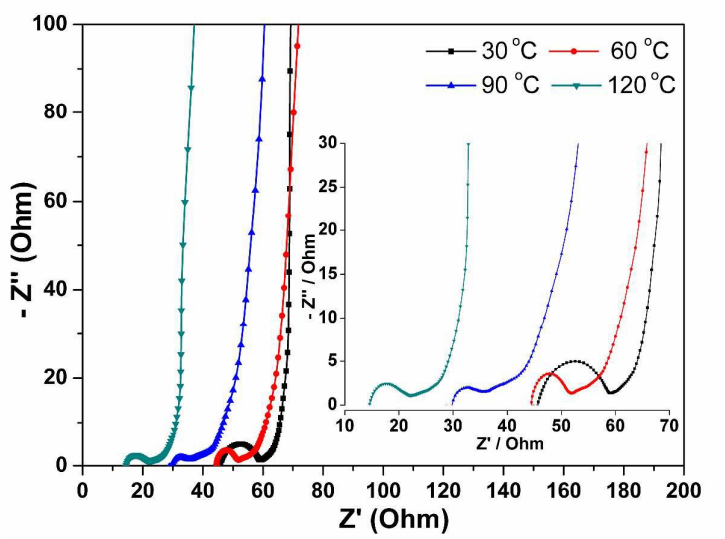

Fig. 6. Nyquist plots of flexible solid-state supercapacitor at different temperature. The inset figure shows the magnified semicircle in the high-frequency region.

The specific capacitances of the solid-state supercapacitor at different temperature are calculated by **Equation (2)** from their respective discharge curve at different current densities and are presented in Fig. 8 (a). The specific capacitances (C_s) are 92.84 F g^{-1}, 94.91 F g^{-1}, 100.38 F g^{-1} and 103.17 F g^{-1} at 30 °C, 60 °C, 90 °C, 120 °C (discharge current density is 0.1 A g^{-1}), respectively. It is noticed that the specific capacitances increase with the temperature increase, the reason is the higher ionic conductivity of the polymer electrolyte at high temperature, and the high ionic conductivity promoting the amount of ions diffuse into electric double layer electrode.[50,52]

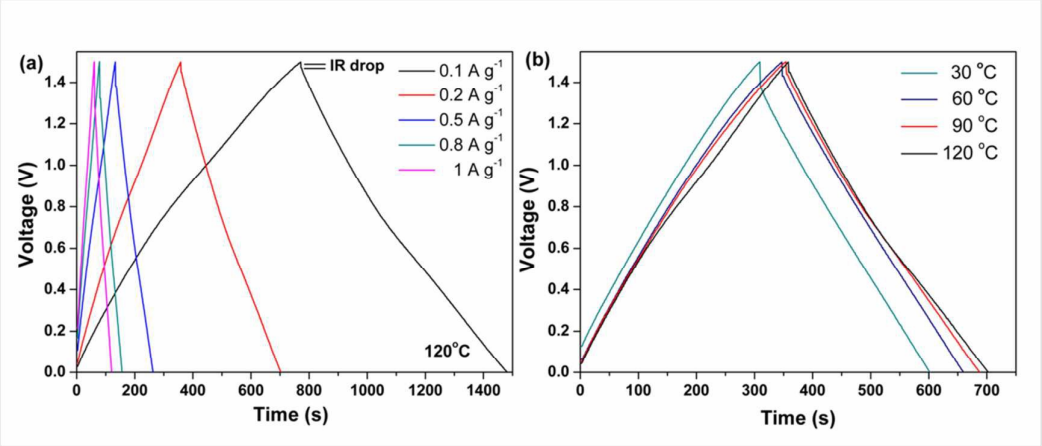

Fig. 7. Galvanostatic charge-discharge curves of the solid-state supercapacitor (a) at various current densities and (b) at different temperature.

With the increasing discharge current density, the specific capacitances decrease slightly at the same temperature, and this tendency is conformed to many previously articles about supercapacitor.[48,50,53] Energy density (E, Wh kg^{-1}) and power density (P, W kg^{-1}) are also two important parameters for evaluating the electrochemical behaviour，which were calculated according to **eqn (3)** and **(4)**. Fig. 8 (b) shows the energy density (E, Wh kg^{-1}) and power density (P, W kg^{-1}) of the supercapacitor at different temperature with various current densities. It is obvious that the supercapacitor at 120 ^{o}C shows the highest energy density of 6.76 Wh kg^{-1} and the power density of 9.55 W kg^{-1} at 0.1 A g^{-1}, and remains the 4.90 Wh kg^{-1} and 81.63 W kg^{-1} at 1 A g^{-1}. For comparison, the energy density and power density for the supercapacitor at 30 ^{o}C is only 1.97 Wh kg^{-1} and 54.73 W kg^{-1} at 1 A g^{-1}, and the energy density of supercapacitor at 120 ^{o}C increased significantly by 148.7% compared to that of the supercapacitor at 30 ^{o}C, the improved electrochemical performances of the supercapacitor at 120 ^{o}C are owed to the higher ionic conductivity of PAEK-PEG based polymer electrolyte at high temperature, and these results agree with the specific capacitances of supercapacitors. In order to make a further comparison with the performance of PAEK-PEG based solid-state supercapacitor, a series of data of supercapacitors in this work with previous values reports are listed in Table 2.

Table 2. Performance comparison of PAEK-PEG based solid-state supercapacitor with different polymer electrolytes from previous literature.

Electrodes materials	Polymer electrolytes	Cs (F g^{-1})	Ereal (Wh kg^{-1})	Voltage (V)	Reference
AC[a]	PAEK-PEG/$LiClO_4$	103.17 (120 °C) 92.84 (30 °C)	6.76 (120 °C) 5.72 (30 °C)	1.5	This work
RGO/f-RGO[a]	Nafion/H_2SO_4	118.5 (RT[c])	-	1	[10]
AC	PAES-Q-1.1[b]	92.79 (RT)	2.61 (RT)	1	[40]
AC	PEO/6 M KOH	90 (RT)	--	1	[54]
Graphene	PVdF-HFP/$BMIMBF_4$[d]	76 (RT)	7.4 (RT)	1.5	[55]

[a] AC represents Activated carbon, RGO represents reduced graphene oxide, f-RGO represents functionalised reduced graphene oxide.

[b] PAES-Q-1.1 separator is prepared by quaternary ammonium functionalized poly(arylene ether sulfone) copolymer in our previous work.

[c] RT represents room temperature.

[d] $BMIMBF_4$ represents 1-Butyl-3-methylimidazolium tetrafluoroborate.

Flexible energy storage devices represent a mainstream direction in modern electronics and related fields, so the capacitive performance of flexible solid-state supercapacitor under different bending conditions were tested by CVs. Fig. 9 (a) shows the cyclic curves of the supercapacitor at different bending angles from 0^o to 120^o, the nearly coincident CVs shapes represent that the bending conditions has no effect on the capacitance performance of the supercapacitor.

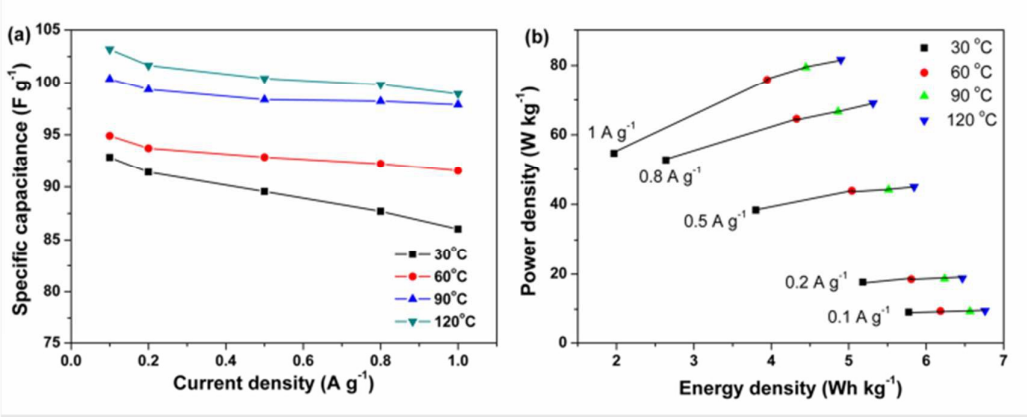

Fig. 8. (a) The specific capacitances and (b) energy and power densities of the supercapacitor at different temperature with various current densities.

The durability performance is also a crucial parameter for all solid-state supercapacitor. In order to evaluate the practical applications of the supercapacitor at high temperature, the cycle life test of the as-fabricated supercapacitor was investigated by repetitious galvanostatic charge-discharge test for 2000 cycles at 120 ^{o}C and 30 ^{o}C, successively. And the current density is 0.5 A g^{-1}. The plots of specific capacitances with increasing cycle numbers are shown in Fig. 9 (b). The initial 500 cycles were carried out at 120 ^{o}C, thereafter, 1000 cycles at 30 °C and last 500 cycles at 120 ^{o}C were carried out, alternatively. After 2000 cycles, the C_s of the supercapacitor has scarcely decrease, which can be concluded that the supercapacitor with solid polymer electrolyte has excellent cyclic stability at extreme high temperature (120 ^{o}C), the inset digital picture shows the solid polymer electrolyte before and after thermal treatment at 120 ^{o}C for 240 h, the solid polymer electrolyte still transparent and colorless after thermal treatment, which further indicates the thermal aging resistance of the solid polymer electrolyte, and proves the excellent practical applications of the supercapacitor at extreme high temperature.

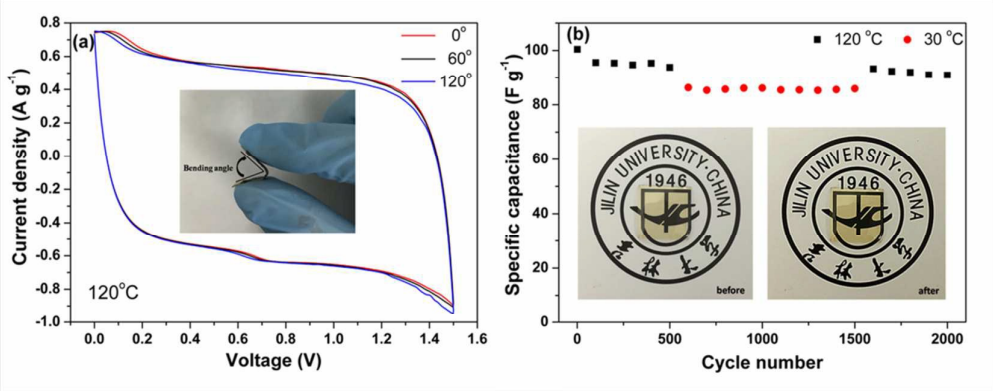

Fig. 9. (a) CV curves of the solid-state supercapacitor measured at various bending states and (b) Change of specific capacitance of supercapacitor with the number of GCD cycles at 30 ^{o}C and 120 ^{o}C. The inset of (b) shows the digital picture of solid polymer electrolyte before and after thermal treatment at 120 ^{o}C for 240 h.

4. Conclusions

In summary, we have successfully synthesized a series of PAEK–PEG copolymers and developed solid polymer electrolyte with high thermal stability and ionic conductivity. Then the high temperature performance PAEK–PEG solid polymer electrolyte based flexible solid-state supercapacitor was fabricated. The nearly rectangular shape of cyclic voltammetry curves and the analogous to an isosceles triangle shape of the galvanostatic charge–discharge curves show the ideal capacitive performance of the supercapacitor, the high specific capacitance of the electrodes (e.g. 103.17 F g^{-1} at 120 ^{o}C) and the high energy density of 6.76 Wh kg^{-1} with a power density of 9.55 W kg^{-1} at 120 ^{o}C also show the high electrochemical performance of the supercapacitor at high temperature. More importantly, the flexible solid-state supercapacitor still remains stability electrochemical performance under different bending state and after 2000 GCD cycles at different temperature, which demonstrated the flexible solid-state supercapacitor obtained in this work may offer a new path for the high temperature energy storage systems.

Acknowledgements

The authors gratefully acknowledge the financial support from the Ph.D. Program Foundation of Ministry of Education of China (No. 20120061110017), Jilin Provincial Science and Technology Development Project of China (20150204001GX), Jilin Provincial Economic Structure Strategic Adjustment Guide Fund Special Project (High Technology Industry) (2015Y045) and Changchun Science and Technology Development Plan Program of China (2013050).

References

1. J.R. Miller, *Science*, 2012, **335**, 1312.
2. F. Liu, S.Y. Song, D.F. Xue and H.J. Zhang, *Adv. Mater*, 2012, **24**, 1089.
3. L. Nyholm, G. Nystrom, A. Mihranyan and M. Strømme, *Adv. Mater*, 2011, **23**, 3751.
4. H. Gwon, H.S. Kim, K.U. Lee, D.H. Seo, Y.C. Park, Y.S. Lee, B.T. Ahn and K. Kang, *Energy Environ. Sci*, 2011, **4**, 1277.
5. Q.Cao, H.S. Kim, N. Pimparkar, J.P. Kulkarnl, C. Wang, M. Shim, K. Rov, M.A. Alam and J.A. Roqers, *Nature*, 2008, **45**, 495.
6. P. Simon and Y. Gogotsi, *Nat. Mater*, 2008, **7**, 845.
7. M.D. Strooler and R.S. Ruoff, *Energy Environ. Sci*, 2010, **3**, 1294.
8. Y.J. Kang, S.J. Chun, S.S. Lee, B.Y. Kim, J.H. Kim, H. Chung, S.Y. Lee and W. Kim, *ACS Nano*, 2012, **6**, 6400.
9. C.L. Lai, Z.P. Zhou, L.F. Zhang, X.X. Wang, Q.X. Zhou, Y. Zhao, Y.C. Wang, X.F. Wu, Z.T. Zhu and H. Fong, *J. Power Sources*, 2014, **247**, 134.
10. B.G. Choi, J. Hong, W.H. Hong, P.T. Hammond and H. Park, *ACS Nano*, 2011, **5**, 7205.
11. A. Burke, *J. Power Sources*, 2000, **91**, 37.
12. R. Kötz and M. Carlen, *Electrochim. Acta*, 2000, **45**, 2483.
13. C.L. Lai, Z.P. Zhou, L.F. Zhang, X.X. Wang, Q.X. Zhou, Y. Zhao, Y.C. Wang, X.F. Wu, Z.T. Zhu and H. Fong, *J. Power Sources*, 2014, **247**, 134.

14. C.Z. Meng, J. Maeng, S.W.M. John and P.P. Irazoqui, *Adv. Energy Mater*, 2013, **7**, 403.
15. X.H. Lu, T. Zhai, X.H. Zhang, Y.Q. Shen, L.Y. Yuan, B. Hu, L. Gong, Y.H. Gao, J. Zhou, Y. Tong and Z.L. Wang, *Adv.Mater*, 2012, **24**, 938.
16. Q. Eliana and M. Piercarlo, *Chem. Soc. Rev*, 2011, **40**, 2525.
17. D. Kalpana, N.G. Renganathan and S. Pitchumani, *J. Power Sources*, 2006, 157, 621.
18. N.A. Choudhury, S. Sampath and A.K. Shukla, *Energy Environ. Sci*, 2009, **2**, 55.
19. C.W. Huang, C.A. Wu, S.S Hou, P.L. Kuo, C.T. Hsieh and H.S. Teng, *Adv. Funct. Mater*, 2012, **22**, 4677.
20. A. M. Stephan and K. S. Nahm , *Polymer*, 2006, **47**, 5952.
21. F.L. Deng, X.E. Wang, D. He, J. Hu, C.L. Gong, Y.S. Ye, X.L. Xie and Z.G. Xue, *J. Memb. Sci*, 2015, 491, 82.
22. W.H. Meyer, *Adv. Mater*, 1998, **10**, 439.
23. Z.G. Xue, D. He, X.L. Xie, *J. Mater. Chem. A*, 2015, **3**, 19218.
24. A. Asghar, Y.A. Samad, B.S. Lalia and R. Hashaikeh, *J. Memb. Sci*, 2012, **421**, 85.
25. P.J. Alarco, Y. Abu-Lebdeh, A. Abouimrane and M. Armand, *Nat. Mater*, 2004, **3**, 476.
26. L.Z. Fan, Y.S. Hu, A.J. Bhattacharyya and J. Maier, *Adv. Funct. Mater*, 2007, **17**, 2800.
27. D. Saikia, S.Y. Hu, Y.J. Chang, J. Fang and L.D. Tsai, *J. Memb. Sci*, 2016, **503**, 59.
28. F.H. Meng and Y. Ding, *Adv. Mater*, 2011, **23**, 4098.
29. S.T. Fei and H.R. Allcock, *J. Power Sources*, 2010, **195**, 2082.
30. S. Jankowsky, M.M. Hiller, R. Stolina and H.D. Wiemhöfer, *J. Power Sources*, 2015, **273**, 574.
31. D.J. Harris, T.J. Bonagamba, K. Schmidt-Rohr, P.P. Soo, D.R. Sadoway, A.M. Mayes, *Macromolecules*, 2002, **35**, 3772.
32. H. Ohno, *Electrochim. Acta*, 2001, **46**, 1407.

33. M. Ueno, N. Imanishi, K. Hanai, T. Kobayashi, A. Hirano, O. Yamamoto and Y. Takeda, *J. Power Sources*, 2011, **196**, 4756.
34. L. A. Guilherme, R. S. Borges, E. M. S. Moraes, G. G. Silva, M. A. Pimenta, A. Marletta and R. A. Silva, *Electrochim. Acta*, 2007, **53**, 1503.
35. G. Zardalidis, E. F. Ioannou, K. D. Gatsouli, S. Pispas, E. I. Kamitsos and G. Floudas, *Macromolecules*, 2015, **48**, 1473.
36. M. Chintapalli, X. C. Chen, J. L. Thelen, A. A. Teran, X. Wang, B. A. Garetz and N. P. Balsara, *Macromolecules*, 2014, **47**, 5424.
37. Q.W. Lu, J.H. Fang, J. Yang, G.W. Yan, S.S. Liu and J.L. Wang, *J. Memb. Sci*, 2013, **425**, 105.
38. M. Kenji, C. Yohei, H. Eiji and W. Masahiro, *J. Am. Chem. Soc*, 2007, **129**, 3879.
39. A.H.N. Rao, R.L. Thankamony, H.J. Kim, S. Nam and T.H. Kim, *Polymer*, 2013, **54**, 111.
40. P.F. Huo, S.L. Zhang, X.R. Zhang, Z. Geng, J.S. Luan and G.B. Wang, *J. Memb. Sci*, 2015, **475**, 562.
41. P.F. Huo, Y. Liu, R.Q. Na, X.R. Zhang, S.L. Zhang and G.B. Wang, *J. Memb. Sci*, 2016, **505**, 148.
42. X.Z. Gu, Y.B. Kuang, X.X. Guo, J.H. Fang and Z.H. Ni, *J Control Release*, 2008, **127**, 267.
43. X.E. Wang, C.L. Gong, D. He, Z.G. Xue, C. Chen, Y.G. Liao and X.L. Xie, *J. Memb. Sci*, 2014, **454**, 298.
44. V.R. Basrur, J. Guo, C. Wang and S.R. Raghavan, *ACS Appl. Mater. Interfaces*, 2013, **5**, 262.
45. P. L. Kuo, C. H. Tsao, C. H. Hsu, S. T. Chen and H. M. Hsu, *J. Memb. Sci*, 2016, **499**, 462.
46. S. Seki, M.A.B.H. Susan, T. Kaneko, H. Tokuda, A. Noda and M. Watanabe, *J. Phys. Chem. B*, 2005, **109**, 3886.
47. K. H. Teoh, C.S. Lim, C. W. Liew, S. Ramesh, *J. Appl. Polym. Sci*, 2016, **133**, 43275.

48. Y.L. Ni'Mah, M.Y. Cheng, J.H. Cheng, J. Rick and B.J. Hwang, *J. Power Sources*, 2015, **278**, 375.
49. J. Rodriguez, E. Navarrete, E.A. Dalchiele, L. Sanchez, J.R. Ramos-Barrado and F. Martin, *J. Power Sources*, 2013, **237**, 270.
50. R. Vellacheri, A. Al-Haddad, H.P. Zhao, W.X. Wang, C.L. Wang and Y. Lei, *Nano Energy*, 2014, **8**, 231.
51. R.S. Hastak, P. Sivaraman, D.D. Potphode, K. Shashidhara and A.B. Samui *Electrochim. Acta*, 2012, **59**, 296.
52. H.J. Fei, C.Y. Yang, H. Bao and G.C Wang, *J. Power Sources*, 2014, **266**, 488.
53. X.H. Lu, G.M. Wang, T. Zhai, M.H. Yu, S.L. Xie, Y.C. Ling, C.L Liang, Y.X. Tong and Y. Li, *Nano Energy*, 2012, **12**, 5376.
54. A. Lewandowski, M. Zajder, E. Frackowiak and F. Beguin, *Electrochim. Acta*, 2001, **46**, 2777.
55. Pandey and A.C. Rastogi, *MRS Proc*, 2012, **1440**, 12.

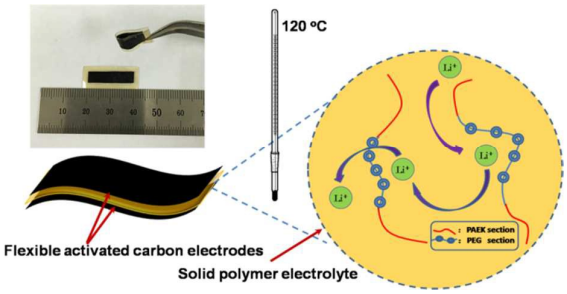

Here in we fabricated a high temperature flexible solid-state supercapacitor based on poly(aryl ether ketone)–poly(ethylene glycol) copolymers solid polymer electrolyte. As fabricated supercapacitor has excellent electrochemical performance and excellent flexibility, outstanding cycle stability at various operating temperature especially high temperature (120 ^{o}C).